The first firn core from Peter 1st Island – capturing climate variability across the Bellingshausen Sea

Elizabeth R. Thomas[1], Dieter Tetzner[1], Bradley Markle[2,3], Joel Pedro[4,5], Guisella Gatacuia[6], Dorothea E. Moser[1,7], Sarah Jackson[8]

[1]Ice Dynamics and Paleoclimate, British Antarctic Survey, High Cross, Madingley Road, Cambridge, CB23 7XT, UK

[2]Department of Geological Sciences, University of Colorado, Boulder, USA

[3]Institute of Arctic and Alpine Science, University of Colorado, Boulder, USA

[4]Australian Antarctic Division, Kingston, Tasmania, 7050, Australia

[5]Australian Antarctic Program Partnership, Institute for Marine and Antarctic Studies, University of Tasmania, Hobart, Tasmania, 7004, Australia

[6]National Centre for Climate Research, Danish Meteorological Institute, Copenhagen, Denmark

[7]Department of Earth Sciences, University of Cambridge, Cambridge CB2 3EQ, UK

[8]Research School of Earth Sciences, Australian National University, Canberra, ACT 2600 Australia

Correspondence to: Elizabeth R. Thomas (lith@bas.ac.uk)

Abstract. Peter 1st Island is situated in the Bellingshausen Sea, a region that has experienced considerable climate change in recent decades. Warming sea surface temperatures and reduced sea ice cover have been accompanied by warming surface air temperature, increased snowfall, and accelerated mass loss over the adjacent ice sheet. Here we present data from the first firn core drilled on Peter 1st Island, spanning the period 2001-2017 CE. The stable water isotope data capture regional changes in surface air temperature, and precipitation (snow accumulation) at the site, which are highly correlated with the surrounding Amundsen-Bellingshausen Seas, and the adjacent Antarctic Peninsula ($r>0.6$, $p<0.05$). The firn core data, together with the unique in-situ data from an automatic weather station, confirms the high skill of the ERA5 reanalysis in capturing daily mean temperature and inter-annual precipitation variability, even over a small Sub-Antarctic Island ~~The unique in-situ data from an automatic weather station, together with the firn core data, confirms the high skill of the ERA5 reanalysis in capturing daily mean temperature and inter-annual precipitation variability, even over a small Sub-Antarctic Island.~~ This study demonstrates the suitability of Peter 1st Island for future deep ice core drilling, with the potential to provide ~~an in~~a valuable archive to explore ice-ocean-atmosphere interactions over decadal to centennial timescales for this dynamic region.

Formatted: Font: Not Italic

1. Introduction:

The Sub-Antarctic Island of Peter 1st (Peter I Øy) is a former shield volcano (154 km^2), almost completely covered by a heavily crevassed ice cap. The islands' location in the Bellingshausen Sea (68°51′05″ S, 90°30′35″ W, Fig. 1), and just 450 km from the coast of West Antarctica, make it a scientifically important site for paleoclimate, ice sheet and oceanographic studies. The island is situated within the seasonal sea ice zone, in a region of the Southern Ocean that has experienced a rapid decline in sea ice cover in recent decades reaching a record low in February 2023 (NSIDC, 2023). The rate of sea ice decline in the Bellingshausen Sea since 1979 is comparable to the rate of ice loss in the Arctic (Parkinson, 2019). Reconstructions from ice cores suggest this recent change is part of a 20th century decline, evident in both proxy and observational based reconstructions (Abram et al., 2010; Porter et al., 2016; Thomas et al., 2019).

The closest landmass is the Antarctic Peninsula (AP) and Ellsworth Land coast, a region that has experienced considerable climate and glaciological change during the 20th century. Surface air temperatures on the AP, recorded at coastal research stations, have increased by as much as 2.5°C since the 1950s (Turner et al., 2005)

constituting the largest warming in the Southern Hemisphere (Siegert et al., 2019). Despite a pause in the warming trend during the 21st century (Turner et al., 2016) ~~warming has resumed to record levels~~temperatures have continued to increase (González-Herrero et al., 2022) and paleoclimate archives suggest the warming trend during the late 20th century was part of a 100-year trend (Royles et al., 2013; Thomas et al., 2009; Thomas. and Tetzner., 2018), that is likely to continue in the future (Li et al., 2018). In addition to the rise in temperature, snowfall has increased dramatically during the 20th century (Thomas et al., 2015; Thomas et al., 2008; Thomas et al., 2017) attributed to changes in atmospheric circulation, sea ice changes and rising surface air temperature (Goodwin et al., 2016; Medley and Thomas, 2019; Porter et al., 2016).

Glaciers along the Bellingshausen Sea and Ellsworth Land coast have retreated in recent decades; (Paolo et al., 2015; Pritchard et al., 2009; Smith et al., 2020). Many glaciers display dynamic thinning and grounding-line retreat that has been attributed to incursions of circumpolar deep water (CDW). The water in the Bellingshausen Sea is amongst the warmest in the Southern Ocean, with measured CDW temperature exceeding 1°C (Jenkins and Jacobs, 2008). The island is situated to the northwest of the Belgica Fan, the culmination of the Belgica Trough, an exceptionally large paleo-ice stream (O Cofaigh et al., 2005). Ice sheet reconstructions suggest that during the L~~l~~ast Glacial Maximum all the modern drainage basins along the Bellingshausen Sea coast were tributaries for a single large ice stream that may have extended to the continental shelf, less than ~200 km from Peter 1st Island. Thus, the location of Peter 1st Island, at the northern edge of the continental shelf, is of significance for both modern and paleoclimate, oceanographic and ice sheet studies.

The first firn core from Peter 1st Island was drilled as part of the Sub-Antarctic Ice Core Expedition (SubICE), one of the projects of the international Antarctic Circumnavigation Expedition (ACE) 2017–2018 (Walton, 2018; Thomas et al., 2021). The aim of this study is to present the chemical and stable water isotope data from the Peter 1st Island ice core to explore its suitability for paleoclimate reconstructions. In addition, we utilise a short instrumental record from an automatic weather station (AWS) from Peter 1st I~~i~~sland to test the skill of the fifth generation of ECMWF reanalysis (ERA5). ERA5 reanalysis provides hourly data at 0.25° resolution (~ 31 km), with consistent near-surface temperature when compared with observations across Antarctica (Zhu et al., 2021). While the resolution of ERA5 may not fully capture local climate and precipitation on Peter 1st Island, the AWS and firn core provide a unique opportunity to evaluate the skill of ERA5 at this site. We will 1) establish the firn core age-scale, 2) evaluate the skill of ERA5 at this island, 3) evaluate the firn core proxies against meteorological parameters from ERA5 and 4) discuss the suitability of this site for future deep ice core drilling.

2. Data and methods:

2.1. Ice core site

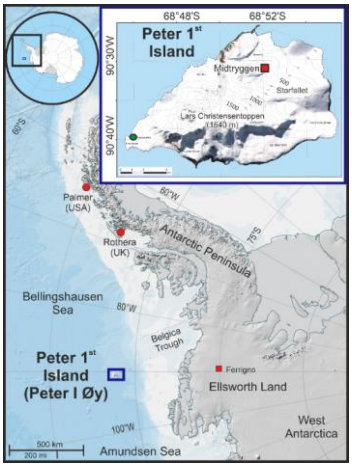

Figure 1: Location of Peter 1st Island (Peter I Øy) in the Bellingshausen Sea, with the ice core site (blue rectangle) with closest Antarctic Peninsula research stations (red circles) and the Ellsworth Land ice core location referenced in the text (Ferrigno, red box). Insert map showing the Peter 1st drilling location (red box), AWS (green dot) and island topography. Map produced using the Antarctic Digital Database, using data made available under the Creative Commons Attribution 4.0 International (CC BY 4.0) licence.

In February 2017 a shallow ice core was drilled to a depth of 12.29 m on Peter 1st Island (68°51′05″ S, 90°30′35″ W). A site had been selected, based on satellite imagery, at the plateau at the top of the island (Lars Christentoppen), however heavy cloud cover prevented helicopter landing at this site. Instead, a lower elevation site was found on a ridge (Midtryggen) at 730 m above sea level, in a small saddle on the eastern side of the island overlooking the main glacier Storfallet (Fig. 1). The snow surface was relatively smooth at this site (slope of ~5°), and ground penetrating radar (GPR) surveys were conducted in a ~500 m radius from the drill site (Thomas et al., 2021). Near continuous stratified layers were observed in the GPR profiles for the upper 43 m at this site (the maximum time window for the GPR) and bedrock was not detected at this depth, however, the full ice thickness has not been determined.

The firn core was drilled using a motorized Kovacs ice-core drill (Mark II) powered by a 4-stroke Honda generator, with core retrieval aided by a sidewinder winch. Ice core sections, with a maximum length of 80 cm, were stored in ethylene-vinyl-acetate-treated (EVA) polythene bags in insulated boxes. The cores were transported to the British Antarctic Survey (BAS) in a -25°C shipping container, and sub-sampled in the -25°C cold laboratories at BAS.

The length and weight of each firn core fragment was measured to calculate density. Based on the measured density profile, and the Herron-Langway model, the estimated bubble close-off depth (when the firn air passages become closed at a density of 0.83 kg m^{-3}) is 34.5 m at this site. Visible melt layers >1 mm thick were recorded (Thomas et al., 2021), revealing an estimated 11% of the ice core is affected by melt, comparable to other Sub-Antarctic and coastal Antarctic ice core sites (Thomas et al., 2021), but considerably less than the Young Island ice core (Moser et al., 2021). Discrete samples were cut at 5 cm resolution for ion-chromatographic (IC) and stable water isotope analysis, sealed in tritan copolyester jars.

2.2. Meteorological data

Meteorological data come from the European Centre for Medium-Range Weather Forecasts (ECMWF) ERA5 analysis (1979–2017) (Copernicus Climate Change Service, 2017), the fifth generation of ECMWF reanalysis. ERA5 reanalysis currently extends back to 1950, providing hourly data at 0.25° resolution (~ 31 km). However, we note that the resolution of ERA5 may not fully capture local climate and precipitation on Peter 1st Island. An AWS was located on the island between February 2006 and January 2007 (http://amrc.ssec.wisc.edu/aws/index.php?region=Ocean%20Islands&station=Peter%20I&year=2006, data downloaded 03/11/2020). The AWS data provides a short (but incomplete) in-situ record of surface temperature (Thomas et al., 2021) covering 149 days between 19th February 2006 and 31st December 2006. This data was not assimilated into the ECMWF model (de Rosnay, 2018). The AWS was located near 68°46.2S, 90°30.3W, at a height of ~128 m on the 'Radiosletta' Plateau on the NW side of the island (Fig.1, insert map). ~~We utilise the observation-based Southern Hemisphere Annular Mode (SAM) Index of (Marshall, 2003) and the Southern Oscillation Index (SOI, defined as the normalized pressure difference between Tahiti and Darwin) of (Ropelewski and Jones, 1987).~~

2.3. Stable water isotopes

Isotopes, $\delta^{18}O$ and δD, were measured using a Picarro L2130-i analyser at the British Antarctic Survey (BAS), with an accuracy of 0.3 and 0.9 ‰ respectively. The measurements are reported against the international standard of Vienna Standard Mean Ocean Water (V-SMOW). Deuterium excess (d_{xs}) is the second-order parameter calculated from the two water isotope ratios ($d_{xs} = \delta D - 8*\delta^{18}O$) (Dansgaard, 1964).

2.4. Major ion chemistry

Major ion concentrations were measured using a high-performance Dionex Integrion ion chromatograph with an injection volume of 250 µL in a class-100 cleanroom at BAS. For the cation chromatograph, we applied a guard column type CS16-4µm (2 × 50 mm) and a CS16-4µm separator column (2 × 250 mm). For the anion chromatograph, we used an AG17-C guard column (2 × 50 mm) together with an AS17-C analytical column (2

× 250 mm). The chemical data presented here is for the purposes of annual layer counting. Ions include sulphate [SO_4^{2-}], methanesulphonic acid [MSA^-], Bromide [Br^-] and Sodium [Na^+], with an analytical precision, defined as the relative standard deviation of the lowest level standard, of 0.03, 0.07, 0.003, and 0.07 ppb respectively.

2.5 Microparticles

Ice samples were filtered through 13 mm diameter, 1.0 µm pore size Whatman™ Polycarbonate membrane filters, inside clean polypropylene Swinnnex™ filter holders. Filters were mounted onto aluminum stubs for analyses on a scanning electron microscope (SEM) at the Earth Sciences Department of the University of Cambridge. Filters were imaged on a Quanta-650F using back scattered electrons on a low-pressure mode. Each filter was imaged at x800 magnification for cryptotephra identification and physical characterization, following the analysis strategy presented in Tetzner et al. (2021).

Formatted: Font: (Default) Times New Roman, 10 pt

Formatted: List Paragraph, Indent: Left: 0.63 cm

2.5. Snow accumulation

The annual snow accumulation is derived from the annual layer thickness (see section 3.1). The thickness is converted to meters of water equivalent (m w_{eq} y^{-1}) based on the measured density. Thinning is corrected using the Nye model, which assumes thinning is proportional to vertical stress, appropriate for the upper 10% of the ice sheet (Nye. 1963). While the ice cap thickness is unknown at this site, GPR confirms that bedrock is at least deeper than 43 m (Thomas et al., 2021). Given the site's elevation (730 m. a.s.l), and the relatively flat surface topography, a depth of 130 m is not unreasonable. While we assume that the 14 m firn core is likely within the upper 10% of the ice cap, and thus suitable for the Nye model (Nye, 1963), we acknowledge that this might not be the most appropriate thinning function for this site.

2.6. Estimating uncertainty and significance

Uncertainty bars of 1 standard error (σ) are applied to all time series, except for 2006 (9.2 m) and ~~2013~~ 2012 (4.5 m) where a 2σ value is applied to account for the influence of melt (section 3.2). For the predicted bottom age estimate (section 4), the uncertainty estimate is calculated based on the difference between an upper and lower snow accumulation estimate. The lower value is based on the snow accumulation derived using all 15 years and the upper value derived with the two high melt years removed.

Statistical significance values (p) applied using a two-tailed T-test. To account for the short duration of the annual data, a bootstrapping method has been applied to find the 95% confidence intervals (Table 1).

3. Results:

3.1. Age-scale

The age-scale has been derived using annual layer counting, based on the $\delta^{18}O$, ~~seasonal deposition of~~ D_{excess} and the seasonal deposition of major ion chemistry (Fig. 2). Clear seasonal cycles are observed D_{EXCESS} as observed at sites in the northern Antarctic Peninsula (Fernandoy et al., 2018). Given its maritime location, seasonal cycles are especially clear in sea salt ions [Na^+] and [Cl^-] and chemical species with marine origin, including [SO_4^{2-}] and [Br^-]. These species relate to changes in marine productivity and sea ice (e.g., Thomas et al., 2019 and references therein), which peak during the phytoplankton bloom in spring and summer. Both [SO_4^{2-}] and [MSA^-] are robust seasonal markers in many coastal Antarctic ice cores (Emanuelsson et al., 2022; Tetzner et al., 2022; Thomas and Abram, 2016), and have also proved to be valuable for dating other sub-Antarctic ice cores (King et al., 2019; Moser et al., 2021).

Summer peaks were assigned if a consistent peak was observed in the D_{excess} (Fig. 2b) and marine ions (Fig. ~~2b~~2c~~-gf~~). The $\delta^{18}O$ ~~stable water isotope~~ record (Fig. 2a) was used as a secondary tracer. An equal number of peaks are identified in the D_{EXCESS}, $\delta^{18}O$ ~~isotope~~ and ions records, however, there is often an offset in the location of the peak. ~~For consistency, the location of the major ion peak was used. Thus, the~~The ~~age~~ location of the peaks is assumed to represent approximately December – November, corresponding to the summer sea ice break-up. The final age-scale ~~extends~~ spans from summer 2017 until summer 2002, encompassing 15 full years.

~~A prominent peak in major ion chemistry (including [SO_4^{2-}]) at 4.6 m depth corresponds to the Puyehue-Cordon Caulle eruption from southern Chile (Fig. 2). This VEI5 rated eruption began in June 2011 and appears in our record from late 2011 and into 2012 and provides at least one independent reference horizon. High biogenic [SO_4^{2-}] background can make identification of volcanic [SO_4^{2-}] peaks difficult, as demonstrated at Antarctic~~

Peninsula sites (Emanuelsson et al., 2022; Tetzner et al., 2021). While the average [SO_4^{2-}] is lower at Peter 1st than many coastal Antarctic sites, the background [SO_4^{2-}] may make identification of bi-polar eruptions difficult, and the presence of volcanic ash (tephra) may be required to identify volcanic tie points in a deeper ice core from this site. The lower end of the age-scale is constrained by the absence of the recently identified Sturge island eruption in 2001 (Tetzner et al., 2021). This Sub-Antarctic eruption has been detected as large shards in other Sub-Antarctic islands (Moser et al., 2021) and the Ellsworth Land coast adjacent to Peter 1st. Although not definitive, if our age-scale extended beyond 2002, we might expect to see some evidence of this eruption at this site.

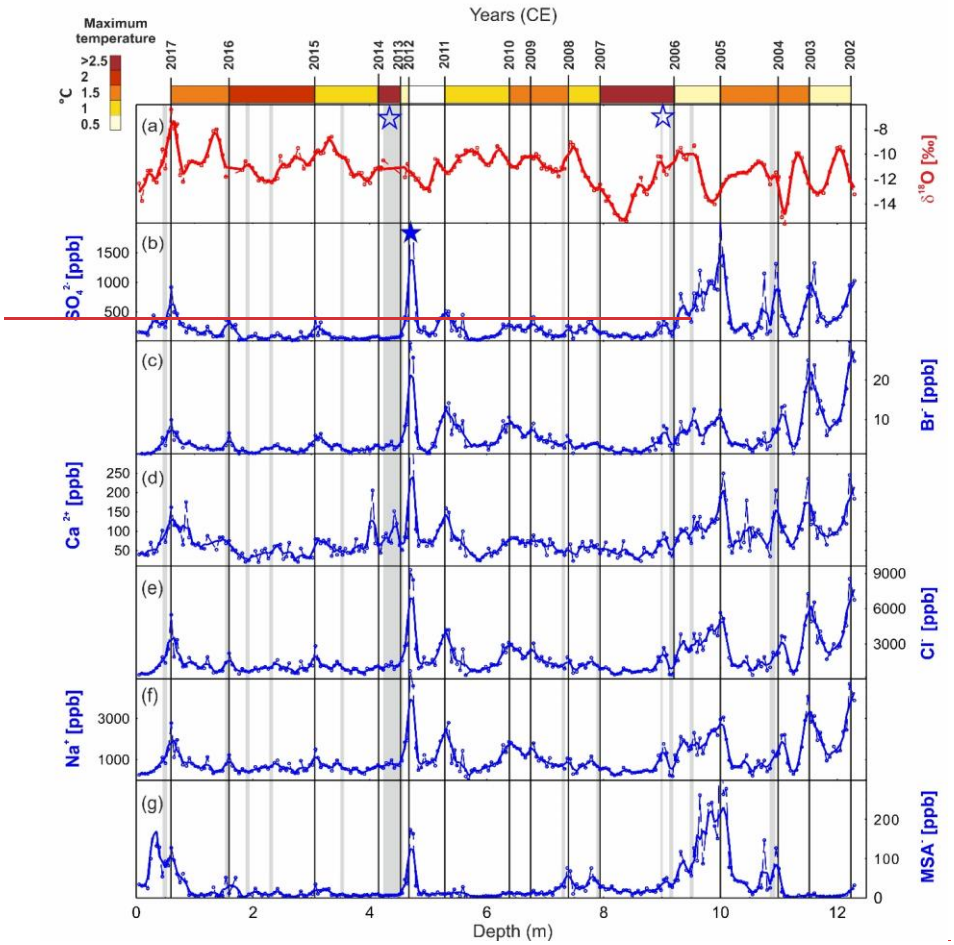
Years (CE)
Maximum temperature
°C
>2.5
2
1.5
1
0.5
2017
2016
2015
2014
2013
2012
2011
2010
2009
2008
2007
2006
2005
2004
2003
2002
(a)
δ18O [‰]
-8
-10
-12
-14
(b)
SO4 2- [ppb]
1500
1000
500
(c)
Br- [ppb]
20
10
(d)
Ca 2+ [ppb]
250
200
150
100
50
(e)
Cl- [ppb]
9000
6000
3000
(f)
Na+ [ppb]
3000
1000
(g)
MSA- [ppb]
200
100
0
0
2
4
6
8
10
12
Depth (m)

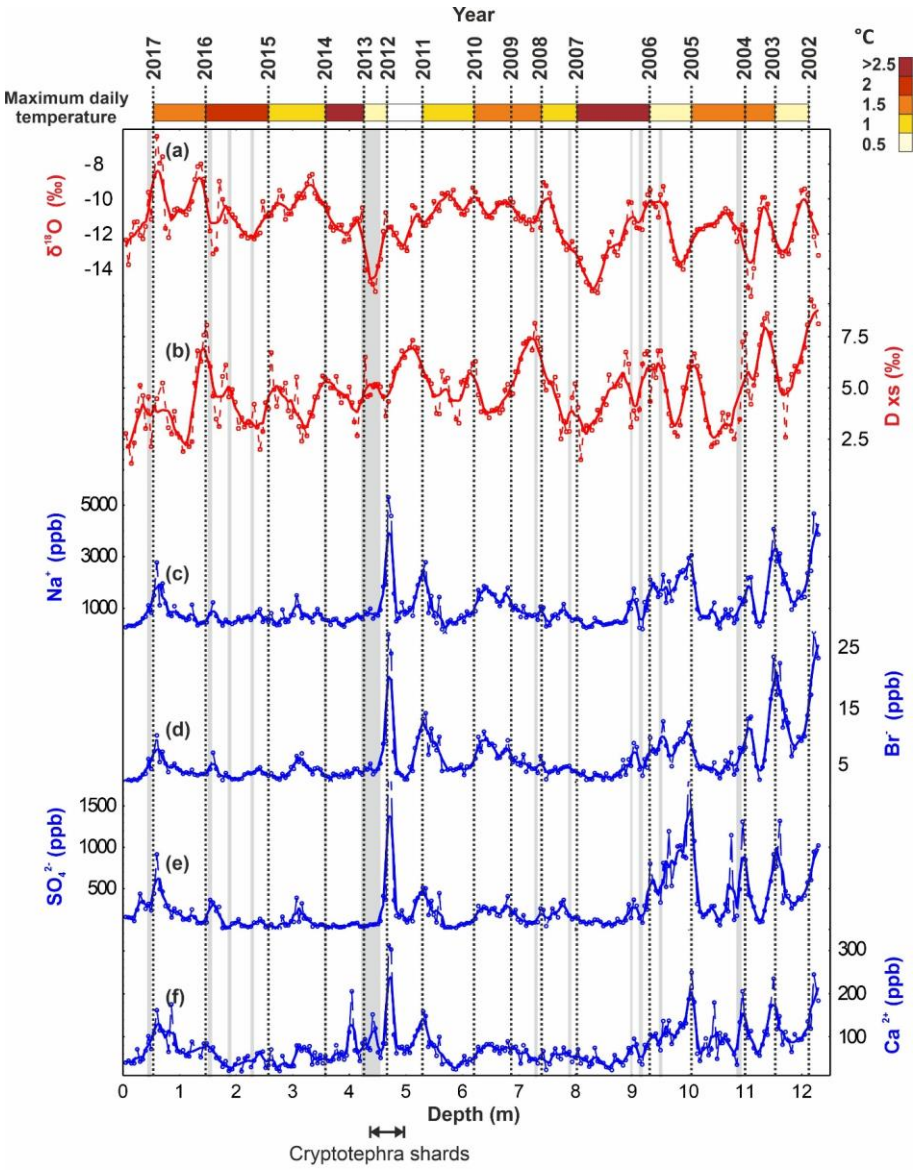

Figure 2: Annual layer counting based on (a) Stable water isotopes ($\delta^{18}O$), (b) deuterium excess (D xs) ~~Sulphate [SO_4^{2-}], (c) Bromide [Br^-], (d) Calcium [Ca^{2+}], (e) Chloride [Cl^-] (f)~~ (c) Sodium [Na^+] (d) Bromide [Br^-], (e) Sulphate [SO_4^{2-}], (f) Calcium [Ca^{2+}], ~~and (g) [MSA^-]~~ all plotted at 5 cm resolution (dashed curves) with a 3-point running mean (solid curves). Vertical dashed black lines indicate the location of summer peaks (approximately January). Vertical grey shading indicates observed melt layers of greater than 5 cm thickness. ~~Open blue stars highlight melt features described in the text and used as reference horizons.~~ Location of cryptotephra shards (Fig. 3) identified in layer

Formatted: Subscript

Formatted: Superscript

corresponding to 2011-2012. **Top colour bar represents the maximum daily 2m temperature (°C) from ERA5, with calendar years above** ~~Solid blue star highlights the peak assigned to the Puyehue-Cordon Caulle eruption in 2011.~~

A prominent peak in major ion chemistry (including $[SO_4^{2-}]$) at 4.6 m depth corresponds to the Puyehue-Cordon Caulle eruption from southern Chile (Fig. 2). This VEI5 rated eruption began in June 2011 and has been observed in a West Antarctic snow-pit during the austral winter of 2011 (Hoffmann et al., 2017). The peak in our record appears in late 2011 and into 2012 and provides at least one independent reference horizon. High biogenic $[SO_4^{2-}]$ background can make identification of volcanic $[SO_4^{2-}]$ peaks difficult, as demonstrated at Antarctic Peninsula sites (Emanuelsson et al., 2022; Tetzner et al., 2021). While the average $[SO_4^{2-}]$ is lower at Peter 1st than many coastal Antarctic sites (Thomas et al., 2023), the background $[SO_4^{2-}]$ may make identification of bi-polar eruptions difficult. The lower end of the age-scale is constrained by the absence of the recently identified Sturge Island eruption in 2001 (Tetzner et al., 2021). This Sub-Antarctic eruption has been detected as large shards in other Sub-Antarctic islands (Moser et al., 2021) and the Ellsworth Land coast adjacent to Peter 1st. Although not definitive, if our age-scale extended beyond 2002, we might expect to see some evidence of this eruption at this site.

Microparticle analysis was included to identify potential cryptotephra shards and provide further evidence for volcanic reference horizons. Distinct shards were observed between 4.6-4.9 m depth, which display sharp edges and a glassy appearance typical of tephra morphology (Fig. 3). The shards appear in the same layer as the $[SO_4^{2-}]$ peak, corresponding to approximately austral winter 2011 to austral autumn 2012. This is consistent with observations from West Antarctica (Koffman et al., 2017). The presence of crypto-tephra shards corresponding to the Puyehue-Cordon Caulle eruption (2011), and the absence of shards corresponding to the Sturge Island eruption (2001), further support our age-scale.

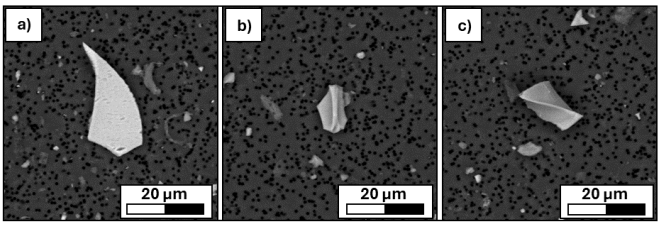

Figure 3: Shards identified from the interval 4.6-4.9 m depth, displaying typical cryptotephra morphology. The images were obtained using a Quanta-650F scanning electron microscope (SEM) at the Earth Sciences Department of the University of Cambridge. Each filter was imaged at x800 magnification using backscattered electron imagery (BSEI) in a low-pressure mode.

An evaluation of the visible melt layers for this site suggests that 11 % of the total ice core is classified as melt (Thomas et al., 2021). This percentage is driven largely by a single 30 cm thick melt layer at a depth of 4.5 m

(Fig. 4a). Based on our annual layer counting, this melt feature corresponds to the year 2012 CE. Over a period of 21 days in January 2013, the daily temperature (ERA5, not corrected for elevation) remained above 0.5°C, reaching a maximum daily temperature of 2.5 °C (Fig. 4b). The prolonged mild conditions in January 2013, likely explain the thick melt feature observed in the year corresponding to 2012 (Fig. 4a). This is a result of the downward percolation of surface meltwater, which has damaged the snow accumulated during the previous autumn and winter (e.g., Moser et al., 2024)

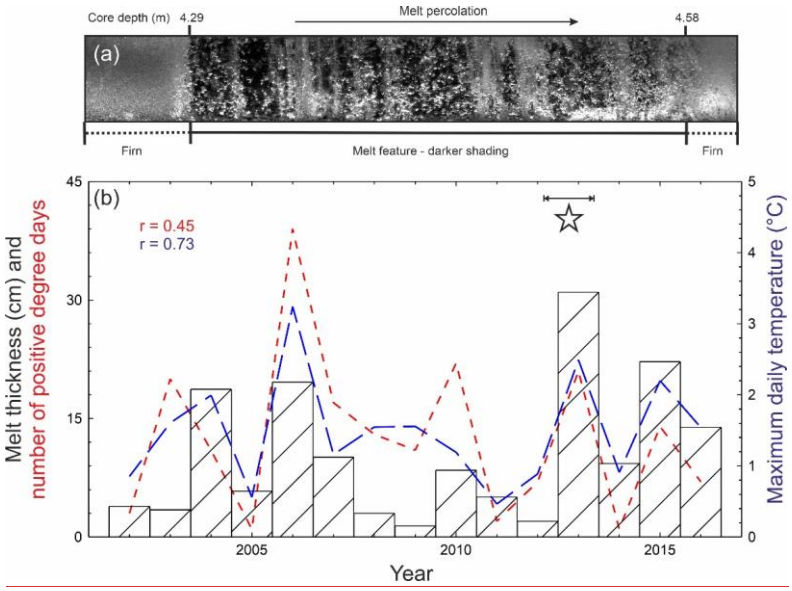

Figure 4. (a) Line scanned image of the Peter 1st firn core. Highlighting the prominent melt feature, observed as a dark area (higher density) between 4.29-4.58 m depth, compared to the lighter shaded (lower density) areas corresponding to firn. (b) Comparison of the annual melt thickness (black bars, cm) in the firn core with the number of positive degree days (red, temperature > 0.5°C) and the maximum daily temperature (blue, °C) from ERA5. Star highlighting the location of the melt feature (a) observed in the 2012 layer, which has been assigned to 2013 due to the downward percolation of meltwater generated during January 2013.

Formatted: Font: Bold

Formatted: Font: Bold

The second most melt effected year is 2006 CE. A maximum daily temperature of 3.2°C (ERA5) was recorded in February 2006, the warmest month in the record. Between February and March 2006, maximum daily temperatures exceeded 0.5°C for a total of 39 days. Positive temperatures during 2006 are corroborated by AWS data, which recorded a maximum daily temperature of 1.94 °C. The down-ward percolation of surface melt is observed in melt features spanning the summer peak corresponding to 2005/2006.

A positive relationship ($r=0.45$, $p<0.1$) is observed between positive degree days (ERA5, temperature > 0.5°C) and annual melt thickness (Fig 4b). The two warmest years on the record, 2006 and 2013 CE, correspond to the most melt affected sections in the core (2006 and 2012), with a significant correlation ($r=0.73$, $p<0.01$) between maximum daily 2m temperature and melt thickness. The alignment of the melt features provides further independent verification for the proposed age-scale.

Formatted: Font: Not Bold

3.2. Evaluating the skill of ERA5 reanalysis to capture temperature

The Peter 1st firn core and the in-situ observations from an AWS provide a unique opportunity to evaluate the skill of the latest generation of reanalysis, ERA5, at a remote Sub-Antarctic Island. The hourly temperature data recorded by the AWS has been converted to daily averages for comparison (Fig. ~~3a~~5a). The AWS recorded intermittently from February to December 2006, and averages were only calculated on days when greater than 50% of the hourly data was available. There is exceptional agreement between the AWS and ERA5 daily data, with a correlation coefficient of r=0.91 for the days of overlap (n=149, p<0.0001). This demonstrates the high degree of skill in the ERA5 reanalysis data, although the period of comparison is short. The average daily temperature from the AWS data was -3.09 °C, 0.93 °C colder than the same days in ERA5. The correlation coefficient is maintained, even when increasing the threshold to only include days when greater than 90% of the hourly data was available (r=0.91, n=105, p<0.0001). However, when only incorporating data above the 90% threshold, the temperature difference between ERA5 and AWS increases to 1.07 °C.

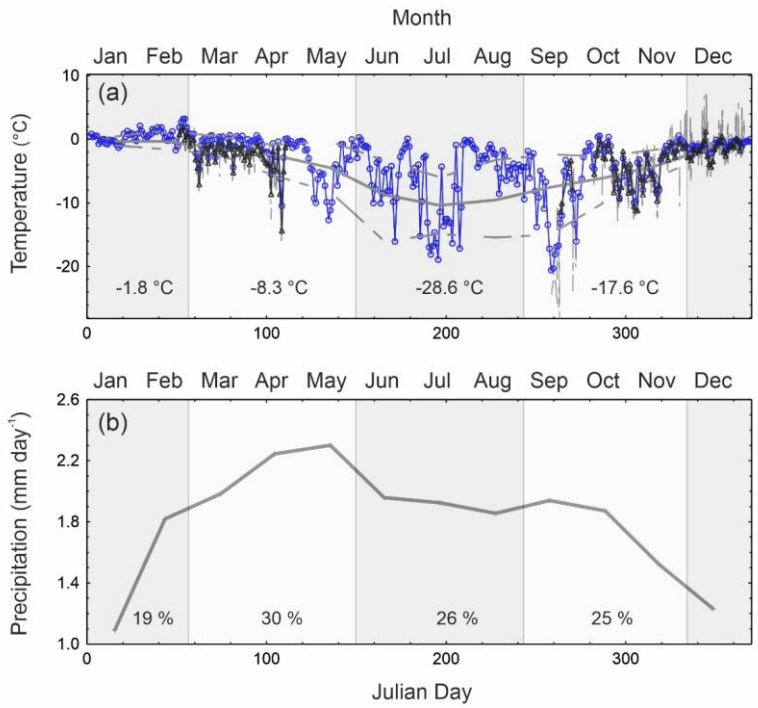

Figure ~~3~~5: Seasonal cycle in temperature (a) and precipitation (b) at Peter 1st Iisland from ERA5 reanalysis (grey curve) (2002-2016 CE). Dashed grey curve represents 2.5 % and 97.5 % percentiles for temperature (a). Daily average temperatures during 2006 CE from ERA5 (blue circle) and AWS (black triangle), with hourly AWS temperature shown in thin grey curve. Grey shading highlights the seasons, with the corresponding average temperature and percentage of precipitation shown. AWS data available from University of Wisconsin-Madison Automatic Weather Station Program.

Due to the adiabatic rate of temperature change of vertically moving air, we would expect slightly colder temperatures at the AWS site (128 m above sea level). A difference of 1.07 ˚C, between the AWS and ERA5 temperatures, would suggest a lapse rate of 0.86° C/ 100m.This is higher than the lapse rate of 0.68°C /100 m

applied in Thomas et al., (2021), based on the measured rate in the western Antarctic Peninsula (Martin and Peel, 1978). However, if a lapse ~~rate of~~rate of 0.86°C is applied to the ERA5 data, this would suggest that maximum daily temperatures at the drill site did not exceed -2.8 °C in the period 2002-2016. This does not fit with the evidence of visible melt features in the firn core.

The appearance of melt features results from a dynamic interplay of atmospheric and snow conditions. However, it is a reasonable assumption that melting will occur when temperatures have exceeded 0 °C, even if only for a few hours. Thus, the discrepancy between ERA5 temperatures and visible melt features in the ice core could suggest that either a lower lapse rate is required, or that ERA5 is cold biased. To test this discrepancy, we explore the relationship between temperature and melt in the firn core.

~~An evaluation of the visible melt layers for this site suggests that 11 % of the total ice core is classified as melt (Thomas et al., 2021). This percentage is driven largely by a single 30 cm thick melt layer at a depth of 4.5 m (Fig. A1). Based on our annual layer counting, constrained by the [SO_4^{2-}] peak at 4.6 m, this melt feature corresponds to the year 2013 CE. Over a period of 21 days in January 2013, the daily temperature (ERA5, not corrected for elevation) remained above 0.5°C, reaching a maximum daily temperature of 2.5 °C (Fig. 2). The prolonged mild conditions likely explain the thick melt feature.~~

~~The second most melt effected year is 2006 CE. A maximum daily temperature of 3.2°C (ERA5) was recorded in February 2006, the warmest month in the record. Between February and March 2006, maximum daily temperatures exceeded 0.5°C for a total of 39 days. Positive temperatures during 2006 are corroborated by AWS data, which recorded a maximum daily temperature of 1.94 °C.~~

If we assume that the melt features corresponding to 2013 ~~(~~captured in the 2012-layer, Fig. 4a) and 2006 CE arose due to positive degree days at the drill site, then we can estimate the lower lapse rate threshold. This is based on the maximum daily temperature in ERA5, during 2013 (2.5 °C) and 2006 (3.2 °C), divided by the difference in elevation at the drill site (730 m). This approach produces a lapse rate estimate of 0.34 - 0.44 °C/ 100 m for 2013 and 2006 respectively, Applying the same approach to the AWS maximum daily temperature (1.94 °C) produces a slightly lower value of 0.32 °C/ 100m. These estimates are at the lower end of the moist adiabatic lapse rate (0.4-0.6 °C/100 m), and lower than lapse rates measured at the Sub-Antarctic Macquarie Island (Fitzgerald and Kirkpatrick, 2020). However, lapse rates as low at 0.31 °C/100 m have been reported at the Sub-Antarctic Marion Island (Nyakatya and McGeoch, 2008).

Applying the estimated lapse rate range, 0.32 to 0.44 °C/100 m, reduces the difference between the AWS and ERA5 temperature from 1.07 °C to 0.67 and 0.52 °C respectively. This is likely a conservative estimate, because 0 °C is the lower limit for melt. However, this suggests that the warmer daily temperatures in ERA5 cannot be explained by differences in elevation alone and may suggest a warm bias in the ERA5 data of between 0.52 to 0.67 °C at this location.

~~A positive relationship is observed between maximum daily 2 m temperatures and melt thickness ($r=0.4$, $p<0.1$). Once the total melt thickness in each year is converted to a melt percentage (dividing the total melt thickness by annual layer thickness), the correlation with 2 m maximum temperatures increases to $r=0.5$ ($p<0.1$). The broad alignment of the melt layers alongside the peaks in chemical species, provide additional evidence for a summer peak. The evidence that the warmest years on the record, 2006 and 2013 CE, correspond to the most melt affected sections in the core provide independent verification for the proposed age-scale.~~

3.3. Evaluating the skill of ERA5 reanalysis to capture precipitation.

In the absence of daily precipitation data from the AWS, we can use the snow accumulation derived from the firn core to evaluate the skill of ERA5 in capturing inter-annual precipitation variability. The average snow accumulation derived from the firn core (2002 – 2016) is 0.49 m weq yr^{-1}. This is slightly lower that the estimated precipitation – evaporation (P-E) value of 0.55 m weq yr^{-1} from ERA5 for this site (Fig. ~~4a~~5a). Case studies on the AP and coastal Ellsworth Land, using the previous generation of reanalysis products (ERA-Interim and ERA-40), suggest that snow accumulation is underestimated by between 0.025 and 0.26 m weq per year (Thomas and Bracegirdle, 2009; Thomas and Bracegirdle, 2015). In this more maritime setting, and

notwithstanding the different orographic positions of the firn core site on the island, there is an offset of approximately 6 cm per year (~12%) between the snow accumulation recorded in the firn core and ERA5 (P-E).

Snow accumulation is the sum of precipitation, evaporation, melt, erosion, and sublimation. Wind driven erosion and re-distribution is estimated to remove between 5-20 cm yr $^{-1}$ of precipitated snow in Antarctic coastal regions (Lenaerts and van den Broeke, 2012), which is within the lower range of our observed offset. In addition, we have already established that this site is influenced by melt, which not only alters the density calculations, but may also suggest potential loss as melt run-off. ~~Removing all years where the percentage of the annual layer thickness classified as melt exceeds 20% (years 2006 and 2013 CE), the revised snow accumulation (0.53 m weq yr^{-1}) is just 2 cm (~4%) lower than the ERA5 P-E.~~

3.4. Snow accumulation

Snow accumulation (2016 – 2002) at Peter 1st is positively correlated with P-E from ERA5. Strong correlations are observed over the island (r=0.75, p<0.01), with an extended zone of correlation (r>0.6) across the Bellingshausen Sea, the Antarctic Peninsula, and the Ronne-Filchner ice shelf (Fig. ~~4b~~6b). ~~This relationship between snow accumulation at Peter 1st and the adjacent Ellsworth Land coast is confirmed by comparison with the snow accumulation record from the Ferrigno ice core drilled in 2010 (Thomas et al., 2015). Despite the short period of overlap (n=9), the two records are positively correlated (r=0.62, p<0.1) with a similar average snow accumulation rate (0.55 m w_{eq} yr^{-1} at Ferrigno).~~

A positive correlation is also observed between snow accumulation and surface air temperature from ERA5 (r=0.~~58~~59, p<0.05). The spatial extent of the correlations (not shown) broadly mirrors the relationship with precipitation (Fig. ~~4b~~6b), extending from the Bellingshausen Sea over the Antarctic Peninsula.

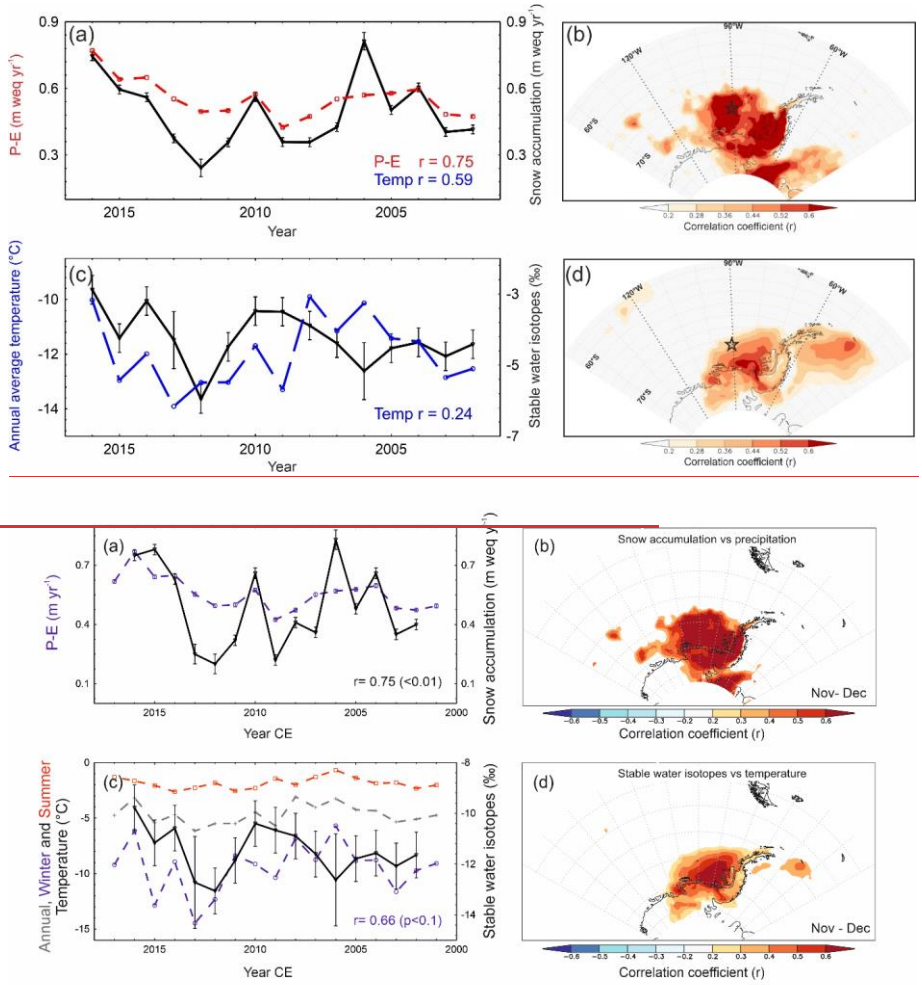

Figure 46: (a) Peter 1st annual average snow accumulation (solid black), compared with precipitation-evaporation (P-E) (dashed blue) from ERA5 reanalysis data (20012002-20172016). Cwith corresponding correlation coefficients (r) value shownfor snow accumulation and P-E (red) and snow accumulation with 2m temperature (blue). (b) Spatial correlation plot of annual snow accumulation with annual ERA5 P-E (all coloured areas p>0.05). (c) Annual average stable water isotope ($\delta^{18}O$) (solid black), compared with annual average 2 m temperatures from ERA5, as annual (grey dashed), summer (red dashed) and winter ((blue dashed) averages. Correlation coefficient (r) between annual $\delta^{18}O$ and winter average 2m temperature after high melt years removedannual average 2 m temperature (blue). (d) Spatial correlation plot of annual $\delta^{18}O$ with annual ERA5 2m temperature (all coloured areas p.0.05). All annual averages calculated as December to November, summer December to March and winter June-August. Uncertainty bars are one standard error (σ), for all years except 2006 and 20132012, where 2σ are applied to account for additional uncertainties relating to melt.

3.5. Stable water isotopes

The stable water isotope composition of Antarctic snowfall has been used to reconstruct past surface temperatures at annual to centennial timescales (e.g., (Stenni et al., 2017) and references therein). However, the processes controlling isotopic composition are complex, relating to water vapour origin, distance from source

(Hatvani et al., 2017), condensation conditions, fractionation pathways (Markle and Steig, 2022), precipitation seasonality, intermittency and post-depositional changes (Münch et al., 2017; Fernandoy et al., 2012).

The annual average stable water isotopes (both $\delta^{18}O$ and δD) at Peter 1st are weakly correlated with ERA5 2 m temperatures at the site ($r=0.37$24, $p>0.1$) (Fig. 4c6c). Removing the two most melt affected years (2013 & 2006 CE) and comparing the annual record with winter average 2m temperature (June–August), increases the correlation with 2 m temperatures to $r=0.61$ ($p<0.05$) (Table 1) and $r=0.66$ ($p<0.05$) respectively.

The relationship between $\delta^{18}O$ and temperature is much stronger over the adjacent ocean (Fig. 4d5d). The spatial correlation plot reveals a strong positive correlation with 2 m temperature over the Bellingshausen Sea ($r>0.6$), within the approximate area of the seasonal sea ice zone.

3.6. Major ions

As expected for an island location, the major ions deposited at Peter 1st are largely of marine origin. The ratio of Cl^-/Na^+ in the ice core is 1.8, consistent with the standard seawater ratio (1.79). Thus, at this site $[Na^+]$ can be considered primarily of marine origin (~95%). The Cl^-/Mg^{2+} and Cl^-/Ca^{2+} ratios suggest that seawater accounts for 82% and 73% of the $[Mg^{2+}]$ and $[Ca^{2+}]$ concentration respectively.

The average $[Na^+]$ at Peter 1st is 998 ppb, consistent with a coastal location. A database of 105 Antarctic ice cores (Thomas et al., 20222023) suggest that the highest $[Na^+]$ in an Antarctic ice core is observed on the Fimbul ice shelf, coastal East Antarctica, where average concentrations exceed 2700 ppb. The average $[Na^+]$ at Peter 1st is higher than the Sub-Antarctic Island of Bouvet, in the South Atlantic, where the average $[Na^+]$ was 101 ppb (King et al., 2019). It is also higher than values on the Antarctic Peninsula, which range between 50-215 ppb (Emanuelsson et al., 2022; Thomas et al., 2022), however, the drill sites are higher in elevation and further from the oceanic source.

The average $[SO_4^{2-}]$ at Peter 1st is 267 ppb. This is considerably higher than concentrations found in Antarctic Peninsula ice cores, where values of between ~30 and 70 ppb are observed (Thomas et al., 20222023; Emanuelsson et al., 2022). However, higher concentrations are observed at Bouvet Island (King et al., 2019) (529 ppb) and the Fimbul ice shelf (536 ppb) (Thomas et al., 20222023).

3.7. Source regions and transport pathways of snowfall

To establish the potential source regions of proxies, and their transport routes to the site, we evaluate the snow accumulation against climate parameters from ERA5 (Table 1). We acknowledge that the short duration of the ice core record may lead to spurious results and thus have generated a "pseudo core" based on the P–E extracted from ERA5 at the firn core location. Spatial correlations are run using the 15 years of firn core data, the same 15-year window (2002 – 2016) for the pseudo core and the extended 37 years (1979 – 2016) of pseudo core data (Fig. 5). We acknowledge that corelations between parameters from the same model domain (ERA5) may be artificially high, while corelations with snow accumulation are expected to be lower due to post-depositional effects (e.g., wind redistribution, sublimation, and melt). However, the aim is to provide longer records for comparison, and establish if the spatial relationships between climate parameters are broadly captured by the firn core data. In recognition of the short duration of the cores, we do not extend this analysis to compare with known climate indices (e.g., SAM or ENSO).

The spatial correlation between snow accumulation (P–E for the pseudo cores) and geopotential height (850 hPa) are shown in figures 5a, 5d and 5g. A distinct pattern of positive correlations is observed over the southern tip of South America and the Drake Passage, with opposing negative correlations over the Atlantic and Indian sectors of the Southern Ocean. The spatial correlations are remarkably similar when using both the firn core derived snow accumulation and the pseudo core data over the same period (Fig. 5d). Over the extended period (1979 – 2016) the positive correlation remains over southern South America, suggesting this feature is robust over the 37-year period (Fig. 5g). However, the region of negative correlations shifts from over the ocean to over the Antarctic continent, in a pattern reminiscent of the Southern Annular Mode (SAM) (Marshall, 2003).

Meridional winds draw warm, moist air from the South Pacific sector of the Southern Ocean as shown by the strong correlations between snow accumulation and meridional winds (blue area in Fig. 5b, 5e and 5h). The blocking high- and low-pressure anomalies to north and south of the AP funnel the air-masses from the Bellingshausen Sea, over the AP and into the Weddell Sea sector. This zonal transport is shown by the

correlations between snow accumulation and westerly winds (red area in Fig. 5c, 5f, and 5i) across the AP. Thus, enhanced precipitation (more snow accumulation) is associated with stronger northerly and westerly winds across the Amundsen and Bellingshausen Seas. This spatial pattern in meridional winds is observed for the firn core period (2002–2016) and maintained over the longer period (1979–2016), suggesting a degree of stability over decadal timescales. However, there is a definite southward shift in the correlations with zonal winds. During the shorter period of the firn core record, the strongest correlations are with winds at the same latitude or slightly south of the island. However, during the extended period (1979–2016) (Fig. 5i) the highest correlations are observed to the north of the island, further away from the coast of West Antarctica.

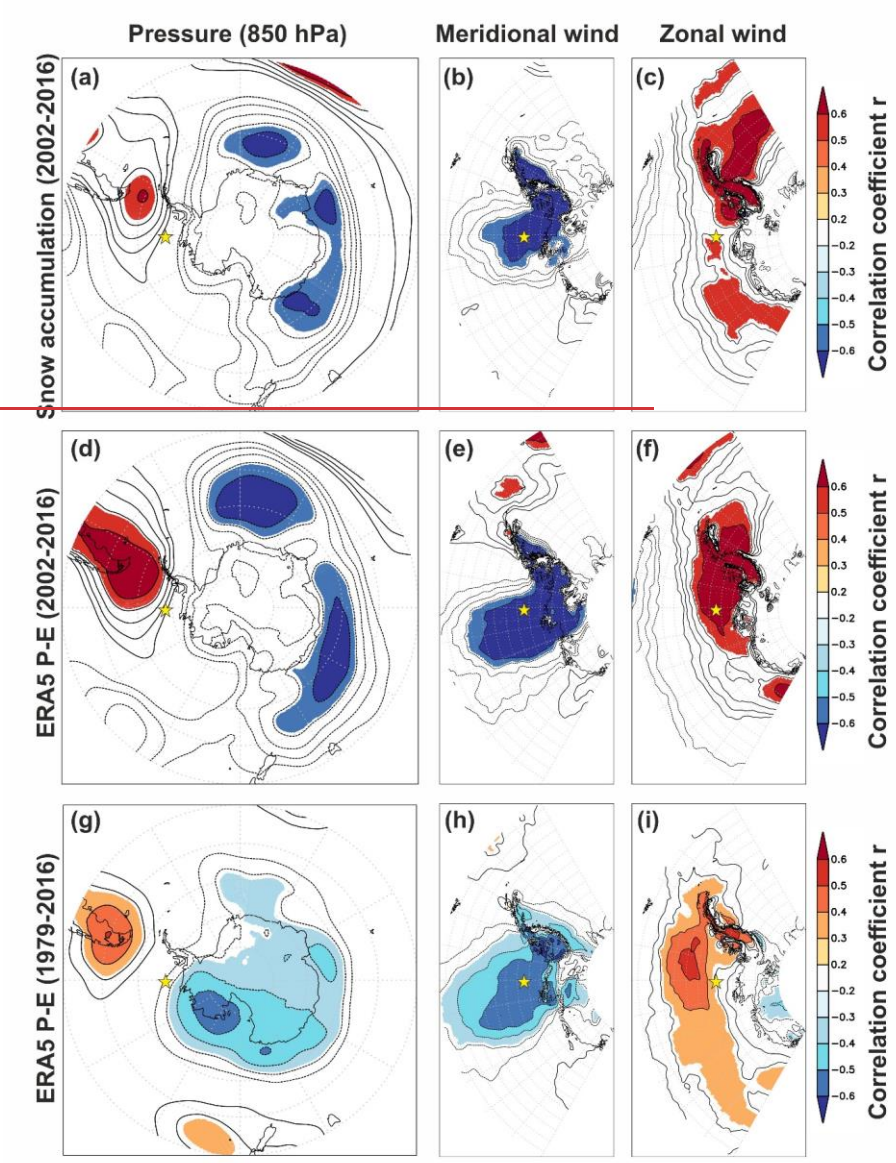

425 **~~Figure 5. Exploring the mechanisms driving precipitation variability at Peter 1st Island (yellow star). Spatial correlation between Peter 1st snow accumulation and (a) geopotential height (850 hPa), (b) meridional winds and (c) zonal winds (ERA5, 2002-2016). Plots d-f are the same spatial correlations but using a timeseries of P-E extracted from ERA5 for the ice core site ("pseudo cores"). Plots g-i are the same but for the extended period 1979—2016.~~**

430

Table 1: Comparing the annual average 2 m temperature (2 m Temp) and P-E data from ERA5 with the annual average stable water isotopes ($\delta^{18}O$) and snow accumulation data (m weq) from the Peter 1st firn core. The 2 m Temp range at the firn core location (730 m a.s.l) is calculated based on a lower lapse rate of 0.32 °C/ 100 m and an upper lapse rate of 0.68 °C/ 100 m (Thomas et al., 2021). Correlation coefficients are shown only if p < 0.05 (n=15). The correlations using all years (n=15) and when the two melt years (2006 & 2013) are removed (n=13), with 95% confidence intervals.

Species		Mean	Max	Min	ERA5 (P-E)		ERA 2m Temp	
	n				r	95%	r	95%
ERA5								
2m Temp (°C)	15	-4.6	-3	-6.2	0.6	0.18-0.83		
2 m Temp (°C)	15	-9.4 to -6.8	-7.8 to -5.3	-11.0 to -8.4	0.6	0.18-0.83		
P-E	15	0.55	0.77	0.43			0.57	0.43-0.73
Peter 1st firn Core								
$\delta^{18}O$ (‰)	15	-11.35 ‰	-6.4 ‰	-15.6 ‰				
	13	-11.15 ‰					0.61	0.56-0.73
Snow accumulation (m weq)	15	0.49	0.83	0.2	0.75	0.71-0.82	0.58	0.44-0.73
	13	0.53	0.77	0.22	0.85	0.84-0.89	0.56	0.41-0.74

4. Discussion:

The objective of this study is to establish if a firn core from Peter 1st Island is suitable for paleoclimate reconstructions. Here we discuss the climatological data captured by the firn core and explore this sites potential for future deep ice core drilling.

4.1. Annual layer counted age-scale.

We have established that seasonal cycles in D_{EXCESS}, major ion chemistry and $\delta^{18}O$ are suitable for annual layer counting. This has been verified using a prominent peak in [SO_4^{2-}]], and evidence for cryptotephra shards, corresponding to the Puyehue-Cordon Caulle eruption in 2011 (Koffman et al., 2017). The lack of evidence (in both [SO_4^{2-}] and crypto tephra) of the Sturge island eruption in 2001, visible at proximal sites on the Antarctic Peninsula (Tetzner et al., 2001), suggests that the this record does not extend beyond 2002. The volcanic reference horizons provide independent age-constraints in approximately the middle (2012) and lower (2002) sections of the firn core.

In addition to the volcanic reference horizons, the location of prominent melt features further supports the age-scale. The two largest melt features occur in the layers assigned to 2013 2012 and 2006, which can be explained by the two warmest years in the ERA5 temperature record (2002-2016) occurring in 2013 and 2006. The downward percolation of meltwater generated in January 2013 means that the melt feature is observed in the annual layer assigned as 2012 (Fig. 4). The AWS data reveals that positive degree days, expected to result in surface melting, did occur for a prolonged period during February and March 2006. The high correlation (r=0.73, p>0.01) between the annual melt layer thickness and maximum daily 2 m temperatures from ERA5 provide further evidence to support the age-scale.

The bottom age of 2002 CE is within the uncertainty range of a previous estimate (2004 +/- 2 years), based on the fitted density profile using the P-E from ERA5 (Thomas et al., 2021). When using the newly calculated snow accumulation (0.49 m weq yr-1), the updated density derived bottom age is 2002 +/- 1 years. Thus, validating the use of the densification model to estimate the potential bottom age for a deeper ice core. The

Formatted: Subscript

Formatted: Superscript

density profile estimate suggests that an ice core drilled to the maximum GPR layer depth (identified at 43 m (Thomas et al., 2021)), would provide a record dating back to 1951.2 CE +/- 5 years. While the ice cap thickness remains unknown, based on the measured snow accumulation rate and density profile, we conclude that an ice core drilled to 100 m depth would provide a record dating back to 1833 CE +/- 13 years.

4.2. Proxy validation and comparison with reanalysis (ERA5)

With only a single AWS temperature record, that does not comprise a full year and is some distance from the ice core site, we must rely on the reanalysis data to evaluate our proxy measurements. The previous ECMWF reanalyses products (ERA-Interim and ERA-40) have been tested widely in Antarctica (e.g., (Bromwich and Fogt, 2004)) and at sites in the adjacent Ellsworth Land coast and the Antarctic Peninsula (Thomas and Bracegirdle, 2009: 2015). A recent study confirms that ERA5 accurately captures variability across Antarctica (Zhu et al., 2021) and in near-surface air temperature and wind regimes over the adjacent Antarctic Peninsula (Tetzner et al., 2019). The AWS data from Peter 1st provides an opportunity to expand this previous research to incorporate a sub-Antarctic Island

The high correlation between daily mean 2 m temperature in ERA5 and temperature recorded in an AWS demonstrate the high degree of skill in ERA5 at this location. The correlation of 0.91 is consistent with the correlation of 0.92 determined when comparing observations and ERA5 annual mean temperatures for Antarctica (Zhu et al., 2021). However, in the absence of a measured lapse rate it is difficult to determine the true temperature bias in the ERA5 reanalysis for Peter 1st. If we apply the lapse rate of 0.32-0.44 °C/100 m (proposed in section 3.2) this suggests that ERA5 has a warm bias of ~0.52-0.67°C.

Comparing the 15 years of annual mean snow accumulation from the firn core with P-E from ERA5 (Fig. 4a) revealed a high temporal correlation between the two records ($r = 0.75$, $p<0.01$; Table 1) and comparable absolute values. The slight over-estimation of the ERA5 total P-E (~ 4-6 %) is less than the offset observed at adjacent sites on the Antarctic Peninsula (Thomas and Bracegirdle, 2009; 2015). Differences between snow accumulation and P-E are expected due to the post-deposition processes including melt and windblown deposition and erosion. In addition, the resolution of the ERA5 reanalysis data (0.25° resolution (~ 31 km)) is not sufficient to differentiate Peter 1st Iisland from the surrounding ocean. However, despite this limitation our study suggests that ERA5 displays a high degree of skill in capturing absolute amount and temporal variability in precipitation changes, at this firn core site on a small and mountainous island location. Importantly, the spatial correlation maps reveal that the high correlation between snow accumulation and ERA5 P-E extends over the Antarctic Peninsula and Amundsen-Bellingshausen Sea region (Fig 4b). These results support the use of the firn core for regional climate reconstructions.

4.3. Relationship between snow accumulation and stable isotopes with precipitation and temperature

The strong correlation ($r=0.75$, $p<0.01$; Table 1) between annual snow accumulation and P-E in the corresponding ERA5 grid cell over the common 15-year interval suggests that the ice core layer thickness (snow accumulation) is dominated by changes in precipitation. Thus, a longer reconstruction could provide valuable insight into changes in snow accumulation and surface mass balance across a large and dynamic region of Antarctica. Although traditionally viewed as a proxy for past surface temperature, the annual average $\delta^{18}O$ at this site is not correlated with site annual average ERA5 2 m temperature (0.3724, $p=0.17$). However, the observed weak correlation coefficients ($\delta^{18}O$ vs 2m surface air temperature) are consistent with ice cores from the Antarctic Peninsula and coastal Ellsworth Land (e.g., Thomas et al., 2009; 2013). ~~The correlation between $\delta^{18}O$ and temperature is improved by removing the melt years and correlated with winter average 2m temperatures. This may suggest that winter conditions play a more dominant role in modulating $\delta^{18}O$ at this site, or that the summer $\delta^{18}O$ signal is weaker or has been lost. The summer months (December – February) receive the lowest amount of snowfall (Fig 3b), just 19% of the total. Thus, the isotopic signal (which is precipitation biased) will be more strongly weighted to the spring, winter, and autumn months respectively. In addition, the summer months may experience more melting, potentially smoothing the isotopic signal of the summer snow deposits~~.

At Peter 1st, the annual snow accumulation is ~~strongly~~ related to annual ERA5 2m surface air temperatures. The positive correlation between snow accumulation and ERA5 2m T ($r=0.6159$, $p<0.0103$) reflects the relationship between temperature and the saturation water vapour pressure governed by the Clausius–Clapeyron relation. This relationship has been observed at ice core sites across the Antarctic Peninsula (e.g., Thomas et al., 2017),

confirmed at the continental scale (Medley and Thomas., 2019) and in a data-assimilation approach using global circulation models (Dalaiden et al., 2021). In the correlation map (Fig. 4d), there is a significant region of correlation between $\delta^{18}O$ and 2 m temperatures over adjacent ocean, especially within the seasonal sea ice zone. This suggests that sea ice may play a role in modulating $\delta^{18}O$ at this site. Sea ice has been shown to directly alter $\delta^{18}O$, through an enrichment of the water vapour (Bromwich and Weaver, 1983). A reduction in the length of the sea ice season and an overall decline in sea ice coverage in the Amundsen and Bellingshausen Seas has been attributed to the warming trends observed in previous West Antarctic reconstructions (Küttel et al., 2012; Steig et al., 2009; Thomas et al., 2013). Thus, we conclude that over longer timescales $\delta^{18}O$ and snow accumulation from any future ice cores from this site will capture changes in surface air temperatures in this region.

4.4. Drivers of variability and the influence of atmospheric modes

The record is too short to draw robust conclusions about the role of large-scale atmospheric circulation. However, given the island's location we expect this site to be strongly influenced by the Amundsen Sea Low (ASL), a climatological low-pressure system that exerts considerable influence on the climate of West Antarctica (Hosking et al., 2013). Pressure in the ASL region is strongly modulated by large-scale modes of variability, especially the Southern Annular Mode (SAM) and El Nino Southern Oscillation ~~and~~ (ENSO) (Fogt et al., 2012; Hosking et al., 2013). Enhanced northerly flow over the Bellingshausen Sea during the positive phase of the SAM has been attributed to the large increase in snowfall on the Antarctic Peninsula during the late 20th century (e.g., Thomas et al., 2008; 2015; 2017; Medley and Thomas, 2019). And back-trajectory analysis suggests that airmasses reaching the Antarctic Peninsula passed over Peter 1st Island (Thomas and Bracegirdle, 2015), suggesting similar climate drivers are likely to influence snowfall at Peter 1st. Given the evidence from back-trajectory analysis, that airmasses reaching the Antarctic Peninsula pass over Peter 1st Island (Thomas and Bracegirdle, 2015), it is likely that the two locations will be influenced by similar climate drivers. ~~The observed relationship between annual snow accumulation at Peter 1st and annual meridional winds over the Bellingshausen Sea replicates the pattern seen at several AP sites (Thomas et al., 2008; 2015; 2017). This shared transport route is confirmed in the back trajectory analysis from the AP sites, which are dominated by air masses that cross directly over Peter 1st Island (Thomas and Bracegirdle, 2015).~~

~~Pressure in the ASL region is strongly modulated by large-scale modes of variability, especially SAM and ENSO (Fogt et al., 2012; Hosking et al., 2013). Despite the short period investigated, the snow accumulation does display significant relationships with both SAM (positive) and ENSO (negative).~~ However, the short duration of the records limits further evaluation of the role of SAM and ENSO, which has been proven to vary temporally at many sites across West Antarctica (Thomas et al., 2015; Wang et al., 2017). ~~During the period captured by the firn core (2002-2016), the SAM has been predominantly in its positive phase, while the period from 1979-2016 is characterised by a shift from negative to positive SAM phase (Marshall, 2003). Indeed, the spatial correlation of annual average P-E from the Peter 1st site (ERA5 "pseudo-core") displays a stronger and more distinct spatial SAM pattern when using the longer record (Fig. 5g) than the period from 2002-2016 captured by the firn core.~~

~~While we might expect the ASL to influence the snow accumulation at Peter 1st, the relationship with snow accumulation and geopotential height in this region is not particularly strong. Instead, the Peter 1st annual snow accumulation (and the pseudo-core data) appears more strongly influenced by the high-pressure anomalies over the Drake Passage, to the north of the AP. Long-lived, and relatively stationary anticyclones have been shown to influence snow accumulation over West Antarctica (Emanuelsson et al., 2018) by impeding the westerly circulation. These anticyclones, also known as blocking events, can deflect marine air towards the Antarctic continent, resulting in increased precipitation. This may also reflect a shift in circulation patterns, as the observed trend toward deeper sea level pressures over the ASL region during the late 20th century has become less pronounced during the early 21st century. Indeed, this shift in circulation patterns has, in part, been attributed to the slowdown in the warming trend observed in the AP (Turner et al., 2016). Therefore, over longer time periods we might expect that snow accumulation from a future deep ice core would capture changes in ASL and blocking event variability.~~

4.5. Drivers of surface melt and the impact on proxy preservation

Despite its maritime location, Peter 1st island is situated south of the polar front at a comparable latitude to much of the East Antarctic coastline (~70°S). While the annual average temperature (1979-2017) is -9.5 °C, with summer temperatures of -5.1 °C (Thomas et al., 2021), the daily temperatures from ERA5 indicate maximum

Field Code Changed

Formatted: Superscript

Formatted: Superscript

Formatted: Superscript

temperature at the site has exceeded 3°C. This maximum in February 2006 was verified by in-situ observations from an AWS. Over the 15-year period (~5500 days) covered by the firn core, there were a total of 189 positive degree days. Many, but not all, of these positive degree days correspond to visible melt layers in the ice core. However, there are some notable exceptions where melt features do not coincide with positive degree days.

Many of the major melt periods also coincide with documented evidence of atmospheric rivers (ARs). These narrow bands of enhanced water vapour transport heat and moisture from the mid- to the high-latitudes and have been attributed to melt events across West Antarctica (Nicolas et al., 2017). Wille et al (2019) derived an AR detection algorithm to demonstrate that between 40-80% of surface melt on the western Antarctic Peninsula (1979-2017) can be attributed to ARs that make landfall during the winter months (March-October). Many of the ARs identified in that study pass directly over Peter 1st Island and may explain the occurrence of visible melt features in the Peter 1st firn core during the winter months (Fig. 2). The yearly percentage of AR occurrences calculated in Wille et al (2019) reveal that two of the most abundant AR years, 2006 and 2013, correspond with the strongest melt features in the firn core. The year 2010 also contained a high number of AR occurrences, however, this year does not correspond to any major melt features in our record. However, 2010 was a high snow accumulation year and the enhanced moisture transport characterised by ARs is also known to increase precipitation. The physical mechanisms relating ARs to surface melt are complex, and thus it may be possible that some ARs passing over Peter 1st result in increased precipitation, but not visible melt features. Or that the ARs during 2010 that made landfall in West Antarctica did not pass directly over Peter 1st Iisland.

There is some evidence that the chemical and isotopic records during the extreme melt event in ~~2013~~ 2012 have been altered. This is observed in the near homogeneous concentrations of major ion and $\delta^{18}O$ values during this melt feature (Fig.2), which appear to have removed the seasonal signal. Meltwater percolation in the firn is known to elute soluble ions and make $\delta^{18}O$ appear smoothed (Moser et al., ~~2023~~2024). The occurrence of melt has also likely increased the uncertainty in the snow accumulation calculations. ~~For example, stronger correlations between snow accumulation (and $\delta^{18}O$) and precipitation (and temperature) are achieved when the two highest melt years (2013 and 2006) are excluded.~~ However, it is only during the most extreme years that melt has had a notable impact on the proxy preservation. A high-resolution evaluation of the melt features, and their impact on chemical elution, is a subject for further study.

Formatted: Superscript

Instrumental records from the Antarctic Peninsula suggest that annual surface air temperatures have increased by approximately 2.5°C since the 1950s (Turner et al., 2005), with reports of record-breaking heatwaves in recent years (González-Herrero et al., 2022). This warming is corroborated by ice core records across the Antarctic Peninsula and coastal Ellsworth Land, which suggest a prominent warming trend during the latter half of the 20th century (Thomas et al., 2013; Thomas et al., 2009; Thomas. and Tetzner., 2018). Despite the absence of a significant warming trend during the 21st century (Turner et al., 2016), the temperatures during the 21st century are still considerably warmer than the early and mid-20th century. Thus, we might expect that the melt frequency observed during this period (2002-2016) will also be much higher than at any time in the recent past. A deeper ice core drilled from this location may be subject to melting in the surface layers, due to continued regional warming (González-Herrero et al., 2022), although the impact of melting is likely limited to the mid-20th century onwards.

This hypothesis is supported by the melt history obtained from the James Ross Island (JRI) ice core, in the north-eastern tip of the Antarctic Peninsula (Abram et al., 2013). Mean annual temperatures of −14.31°C were reported at the JRI site during the 1980s (Aristarain et al., 1987) however, during the period 2001-2017 the annual average temperature increased to -7.5°C, warmer than the -9.5°C observed at Peter 1st. This may explain why the average melt layer thickness of 3.2 cm per year at JRI is higher than the observed 1.8 cm per year at Peter 1st. The visible melt features at JRI display a clear acceleration in frequency during the late 20th century (Abram et al., 2013). However, this melt has not had a notable influence on the proxy preservation or subsequent paleoclimate reconstructions generated from this site (e.g., Abram et al., 2013).

5. Conclusions:

Here we present the first climatic interpretation of $\delta^{18}O$, and snow accumulation data contained in a firn core drilled on the remote sub-Antarctic Island of Peter 1st. We conclude that a deep ice core from this site has the potential to provide valuable paleoclimate reconstructions, exploring the ice-atmosphere-ocean interactions in the Bellingshausen Sea based on the following findings:

- The firn core can be annually layer counted and verified using a volcanic reference horizon from the Puyehue-Cordón Caulle eruption in 2011.
- The ERA5 reanalysis displays a high degree of skill at reproducing site surface temperature and snow accumulation. This is confirmed by comparing daily temperatures from an AWS against ERA5 2-m temperatures and by comparing annual average snow accumulation from the ice core against annual average precipitation (P-E) from ERA5 at the corresponding grid cell. Thus, demonstrating that ERA5 can capture climate variability even at a small sub-Antarctic Island and supporting the use of ERA5 as a suitable dataset to interpret climate proxies in this firn core.
- Snow accumulation observed in the firn core is significantly correlated to both regional precipitation (P-E) changes and changes in surface air temperature.
- Snow accumulation at the firn core site is likely related to large-scale modes of atmospheric variability, including SAM. However, the stability of the relationship between SAM and snow accumulation cannot be confirmed beyond the 15-year interval of the firn core.
- The $\delta^{18}O$ record, although weakly correlated with site temperature, displays a ~~strong and significant~~ relationship with air temperature over the seasonal sea ice zone in the Bellingshausen Sea.
- The melt frequency is lower than observed at existing deep ice core sites from coastal Antarctica. The melt features ~~broadly correspond to~~correlate with maximum daily temperature, with the two most extreme melt years (2006 and ~~2013~~2012) coincident with high temperatures and the documented occurrence of atmospheric rivers (in 2006 and 2013).
- While the ice cap thickness remains unknown, based on the measures snow accumulation rate and density profile we conclude that an ice core drilled to 100 m depth would capture climate variability of the past ~200-years.

Appendices:

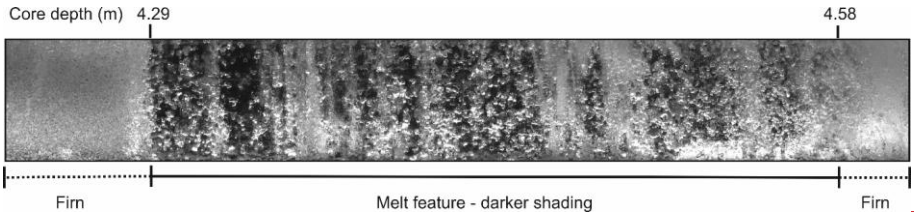

~~**Figure A1: Line scanned image of the Peter 1st firn core. Highlighting the prominent melt feature, observed as a dark area (higher density) between 4.29-4.58 m depth, compared to the lighter shaded (lower density) areas corresponding to firn.**~~

Data availability:

All data is submitted to the UK polar data centre (DOI pending) or available on request (lith@bas.ac.uk).

Author contributions:

ET designed the project and prepared the manuscript with contributions from all authors. JP, BM, GG conducted the fieldwork, DT produced the age-scale, DM contributed to the sample preparation, SJ conducted the IC analysis.

Competing interest:

ET is an editor of Climate of the Past. The peer-review process was guided by an independent editor, and the authors have also no other competing interests to declare."

Acknowledgements:

Funding was provided to subICE by École Polytechnique Fédérale de Lausanne, the Swiss Polar Institute, and Ferring Pharmaceuticals Inc. ERT received core funding from the Natural Environment Research Council to the British Antarctic Survey's Ice Dynamics and Palaeoclimate programme. Joel B. Pedro acknowledges support from the European Research Council under the European Community's Seventh Framework Programme (FP7/2007e2013) and ERC grant agreement 610055 as part of the ice2ice project and from the Australian Government Department of Industry Science Energy and Resources, grant ASCI000002. We are grateful to the Norwegian Polar Institute for granting us permission to visit Peter 1st Island. The authors appreciate the support of the University of Wisconsin-Madison Automatic Weather Station Program for the data set, data display, and information, NSF grant number 1924730 and ECMWF for providing ERA5 reanalysis data. We thank Laura Gerish (BAS) for producing the maps. We thank Joe Brown and Daniel Emanuelsson for the line scanning image presented in A1. Data used in this study are available through the UK Polar Data Centre. The authors would like to acknowledge the coordinators and participants of the Antarctic Circumnavigation Expedition for facilitating collection of the subICE cores, especially David Walton, Christian de Marliave, Julia Schmale, Robert Brett, Sergio Rodrigues, Francois Bernard, Amy King, Roger Stilwell, and Frederick Paulsen.

References:

Abram NJ, Mulvaney R, Wolff EW, et al. (2013) Acceleration of snow melt in an Antarctic Peninsula ice core during the twentieth century. *Nature Geoscience* 6(5): 404-411.

Abram NJ, Thomas ER, McConnell JR, et al. (2010) Ice core evidence for a 20th century decline in sea ice in the Bellingshausen Sea, Antarctica. *Journal of Geophysical Research* 115(D23).

Aristarain AJ, Pinglot JF and Pourchet M (1987) Accumulation and Temperature Measurements on the James Ross Island Ice Cap, Antarctic Peninsula, Antarctica. *Journal of Glaciology* 33(115): 357-362.

Bromwich DH and Fogt RL (2004) Strong Trends in the Skill of the ERA-40 and NCEP–NCAR Reanalyses in the High and Midlatitudes of the Southern Hemisphere, 1958–2001. *Journal of Climate* 17(23): 4603-4619.

Bromwich DH and Weaver CJ (1983) Latitudinal displacement from main moisture source controls δ18O of snow in coastal Antarctica. *Nature* 301(5896): 145-147.

Dalaiden Q, Goosse H, Rezsöhazy J, et al. (2021) Reconstructing atmospheric circulation and sea-ice extent in the West Antarctic over the past 200 years using data assimilation. *Climate Dynamics*. DOI: 10.1007/s00382-021-05879-6.

de Rosnay P (2018) T. Haiden, M. Dahoui, B. Ingleby, P. de Rosnay, C. Prates, E. Kuscu, T. Hewson, L. Isaksen, D. Richardson, H. Zuo, L. Jones.

Emanuelsson BD, Bertler NAN, Neff PD, et al. (2018) The role of Amundsen–Bellingshausen Sea anticyclonic circulation in forcing marine air intrusions into West Antarctica. *Climate Dynamics* 51(9): 3579-3596.

Emanuelsson BD, Thomas ER, Tetzner DR, et al. (2022) Ice Core Chronologies from the Antarctic Peninsula: The Palmer, Jurassic, and Rendezvous Age-Scales. *Geosciences* 12(2): 87.

Fernandoy F, Meyer H and Tonelli M (2012) Stable water isotopes of precipitation and firn cores from the northern Antarctic Peninsula region as a proxy for climate reconstruction. *The Cryosphere* 6(2): 313-330.

Fernandoy, F., Tetzner, DR., Meyer, H., Gacitúa, G., Hoffmann, K., Falk, U., Lambert, F., and MacDonell, S (2018) New insights into the use of stable water isotopes at the northern Antarctic Peninsula as a tool for regional climate studies, *The Cryosphere*, 12, 1069–1090, https://doi.org/10.5194/tc-12-1069-2018, 2018

Fitzgerald NB and Kirkpatrick JB (2020) Air temperature lapse rates and cloud cover in a hyper-oceanic climate. *Antarctic Science* 32(6): 440-453.

Fogt RL, Jones JM and Renwick J (2012) Seasonal zonal asymmetries in the Southern Annular Mode and their impact on regional temperature anomalies. *Journal of Climate* 25(18): 6253-6270.

González-Herrero S, Barriopedro D, Trigo RM, et al. (2022) Climate warming amplified the 2020 record-breaking heatwave in the Antarctic Peninsula. *Communications Earth & Environment* 3(1): 122.

Goodwin BP, Mosley-Thompson E, Wilson AB, et al. (2016) Accumulation Variability in the Antarctic Peninsula: The Role of Large-Scale Atmospheric Oscillations and Their Interactions. *Journal of Climate* 29(7): 2579-2596.

Formatted: Font: Italic

Hatvani IG, Leuenberger M, Kohán B, et al. (2017) Geostatistical analysis and isoscape of ice core derived water stable isotope records in an Antarctic macro region. *Polar science* 13: 23-32.
Hosking JS, Orr A, Marshall GJ, et al. (2013) The Influence of the Amundsen–Bellingshausen Seas Low on the Climate of West Antarctica and Its Representation in Coupled Climate Model Simulations. *Journal of Climate* 26(17): 6633-6648.
Jenkins A and Jacobs S (2008) Circulation and melting beneath George VI Ice Shelf, Antarctica. *Journal of Geophysical Research: Oceans* 113(C4).
King ACF, Thomas ER, Pedro JB, et al. (2019) Organic Compounds in a Sub-Antarctic Ice Core: A Potential Suite of Sea Ice Markers. *Geophysical Research Letters* 46(16): 9930-9939.
Koffman, B. G., Dowd, E. G., Osterberg, E. C., Ferris, D. G., Hartman, L. H., Wheatley, S. D., Kurbatov, A. V., Wong, G. J., Markle, B. R., Dunbar, N. W., Kreutz, K. J., & Yates, M. (2017). Rapid transport of ash and sulfate from the 2011 Puyehue-Cordón Caulle (Chile) eruption to West Antarctica. J. Geophys. Res. Atmos., 122. https://doi.org/10.1002/2017JD026893
Küttel M, Steig EJ, Ding Q, et al. (2012) Seasonal climate information preserved in West Antarctic ice core water isotopes: relationships to temperature, large-scale circulation, and sea ice. *Climate Dynamics* 39(7): 1841-1857.
Lenaerts JTM and van den Broeke MR (2012) Modeling drifting snow in Antarctica with a regional climate model: 2. Results. *Journal of Geophysical Research: Atmospheres* 117(D5).
Li C, Michel C, Seland Graff L, et al. (2018) Midlatitude atmospheric circulation responses under 1.5 and 2.0 C warming and implications for regional impacts. *Earth System Dynamics* 9(2): 359-382.
Markle BR and Steig EJ (2022) Improving temperature reconstructions from ice-core water-isotope records. *Clim. Past* 18(6): 1321-1368.
Marshall GJ (2003) Trends in the Southern Annular Mode from Observations and Reanalyses. *Journal of Climate* 16(24): 4134-4143.
Martin PJ and Peel DA (1978) The Spatial Distribution of 10 m Temperatures in the Antarctic Peninsula. *Journal of Glaciology* 20(83): 311-317.
Medley B and Thomas ER (2019) Increased snowfall over the Antarctic Ice Sheet mitigated twentieth-century sea-level rise. *Nature Climate Change* 9(1): 34-39.
Moser DE, Jackson S, Kjær HA, et al. (2021) An Age Scale for the First Shallow (Sub-)Antarctic Ice Core from Young Island, Northwest Ross Sea. *Geosciences* 11(9): 368.
Moser, DE, Thomas, ER. , Nehrbass-Ahles, C, Eichler, A, Wolff, E. (2024) Melt-Affected Ice Cores for Polar Research in a Warming World. *The Cryosphere*, 18. 28 pp. 10.5194/tc-18-2691-2024~~Moser, DE., Thomas, ER., Nehrbass-Ahles, C., Eichler, A., and Wolff, E.: Review article: Melt-Affected Ice Cores for (Sub-)Polar Research in a Warming World, EGUsphere [preprint~~], https://doi.org/10.5194/egusphere-2023-1939, 2023
Münch T, Kipfstuhl S, Freitag J, et al. (2017) Constraints on post-depositional isotope modifications in East Antarctic firn from analysing temporal changes of isotope profiles. *The Cryosphere* 11(5): 2175-2188.
Nicolas JP, Vogelmann AM, Scott RC, et al. (2017) January 2016 extensive summer melt in West Antarctica favoured by strong El Niño. *Nature Communications* 8(1): 15799.
Nyakatya M and McGeoch MA (2008) Temperature variation across Marion Island associated with a keystone plant species (Azorella selago Hook.(Apiaceae)). *Polar Biology* 31(2): 139-151.
Ó Cofaigh, C., Larter, R. D., Dowdeswell, J. A., Hillenbrand, C.-D., Pudsey, C. J., Evans, J., and Morris, P. (2005), Flow of the West Antarctic Ice Sheet on the continental margin of the Bellingshausen Sea at the Last Glacial Maximum, J. Geophys. Res., 110, B11103, doi:10.1029/2005JB003619.
Paolo FS, Fricker HA and Padman L (2015) Volume loss from Antarctic ice shelves is accelerating. *Science* 348(6232): 327-331.
Parkinson CL (2019) A 40-y record reveals gradual Antarctic sea ice increases followed by decreases at rates far exceeding the rates seen in the Arctic. *Proceedings of the National Academy of Sciences* 116(29): 14414-14423.
Porter SE, Parkinson CL and Mosley-Thompson E (2016) Bellingshausen Sea ice extent recorded in an Antarctic Peninsula ice core. *Journal of Geophysical Research: Atmospheres* 121(23): 13,886-813,900.
Pritchard HD, Arthern RJ, Vaughan DG, et al. (2009) Extensive dynamic thinning on the margins of the Greenland and Antarctic ice sheets. *Nature* 461(7266): 971-975.
Ropelewski CF and Jones PD (1987) An Extension of the Tahiti–Darwin Southern Oscillation Index. *Monthly Weather Review* 115(9): 2161-2165.
Royles J, Amesbury Matthew J, Convey P, et al. (2013) Plants and Soil Microbes Respond to Recent Warming on the Antarctic Peninsula. *Current Biology* 23(17): 1702-1706.
Siegert M, Atkinson A, Banwell A, et al. (2019) The Antarctic Peninsula Under a 1.5°C Global Warming Scenario. *Frontiers in Environmental Science* 7.

Smith B, Fricker HA, Gardner AS, et al. (2020) Pervasive ice sheet mass loss reflects competing ocean and atmosphere processes. *Science* 368(6496): 1239-1242.
Steig EJ, Schneider DP, Rutherford SD, et al. (2009) Warming of the Antarctic ice-sheet surface since the 1957 International Geophysical Year. *Nature* 457(7228): 459-462.
Stenni B, Curran MAJ, Abram NJ, et al. (2017) Antarctic climate variability on regional and continental scales over the last 2000 years. *Clim. Past* 13(11): 1609-1634.
Tetzner D, Thomas E and Allen C (2019) A Validation of ERA5 Reanalysis Data in the Southern Antarctic Peninsula—Ellsworth Land Region, and Its Implications for Ice Core Studies. *Geosciences* 9(7): 289.
Tetzner DR, Allen CS and Thomas ER (2022) Regional variability of diatoms in ice cores from the Antarctic Peninsula and Ellsworth Land, Antarctica. *The Cryosphere* 16(3): 779-798.
Tetzner DR, Thomas ER, Allen CS, et al. (2021) Evidence of Recent Active Volcanism in the Balleny Islands (Antarctica) From Ice Core Records. *Journal of Geophysical Research: Atmospheres* 126(23): e2021JD035095.
Thomas ER and Abram NJ (2016) Ice core reconstruction of sea ice change in the Amundsen-Ross Seas since 1702 A.D. *Geophysical Research Letters* 43(10): 5309-5317.
Thomas ER, Allen CS, Etourneau J, et al. (2019) Antarctic Sea Ice Proxies from Marine and Ice Core Archives Suitable for Reconstructing Sea Ice over the Past 2000 Years. *Geosciences* 9(12): 506.
Thomas ER and Bracegirdle TJ (2009) Improving ice core interpretation using in situ and reanalysis data. *Journal of Geophysical Research: Atmospheres* 114(D20).
Thomas ER and Bracegirdle TJ (2015) Precipitation pathways for five new ice core sites in Ellsworth Land, West Antarctica. *Climate Dynamics*. DOI: 10.1007/s00382-014-2213-6.
Thomas ER, Bracegirdle TJ, Turner J, et al. (2013) A 308 year record of climate variability in West Antarctica. *Geophysical Research Letters* 40(20): 5492-5496.
Thomas ER, Dennis PF, Bracegirdle TJ, et al. (2009) Ice core evidence for significant 100-year regional warming on the Antarctic Peninsula. *Geophysical Research Letters* 36(20).
Thomas ER, Gacitúa G, Pedro JB, et al. (2021) Physical properties of shallow ice cores from Antarctic and sub-Antarctic islands. *The Cryosphere* 15(2): 1173-1186.
Thomas ER, Hosking JS, Tuckwell RR, et al. (2015) Twentieth century increase in snowfall in coastal West Antarctica. *Geophysical Research Letters* 42(21): 9387-9393.
Thomas ER, Marshall GJ and McConnell JR (2008) A doubling in snow accumulation in the western Antarctic Peninsula since 1850. *Geophysical Research Letters* 35(1).
Thomas ER, van Wessem JM, Roberts J, et al. (2017) Regional Antarctic snow accumulation over the past 1000 years. *Clim. Past* 13(11): 1491-1513.
Thomas, E. R., Vladimirova, D. O., Tetzner, D. R., Emanuelsson, B. D., Chellman, N., Dixon, D. A., Goosse, H., Grieman, M. M., King, A. C. F., Sigl, M., Udy, D. G., Vance, T. R., Winski, D. A., Winton, V. H. L., Bertler, N. A. N., Hori, A., Laluraj, C. M., McConnell, J. R., Motizuki, Y., Takahashi, K., Motoyama, H., Nakai, Y., Schwanck, F., Simões, J. C., Lindau, F. G. L., Severi, M., Traversi, R., Wauthy, S., Xiao, C., Yang, J., Mosely-Thompson, E., Khodzher, T. V., Golobokova, L. P., and Ekaykin, A. A.(2023) Ice core chemistry database: an Antarctic compilation of sodium and sulfate records spanning the past 2000 years, Earth Syst. Sci. Data, 15, 2517-2532, 10.5194/essd-15-2517-2023, 2023.
~~Thomas ER, Vladimirova DO, Tetzner DR, et al. (2022) Ice core chemistry database: an Antarctic compilation of sodium and sulphate records spanning the past 2000 years. *Earth Syst. Sci. Data Discuss.* 2022: 1-20.~~
Thomas. E, R and Tetzner. D, R. (2018) The Climate of the Antarctic Peninsula during the Twentieth Century: Evidence from Ice Cores. DOI: 10.5772/intechopen.81507.
Turner J, Colwell SR, Marshall GJ, et al. (2005) Antarctic climate change during the last 50 years. *International Journal of Climatology* 25(3): 279-294.
Turner J, Lu H, White I, et al. (2016) Absence of 21st century warming on Antarctic Peninsula consistent with natural variability. *Nature* 535(7612): 411-415.
Zhu J, Xie A, Qin X, et al. (2021) An Assessment of ERA5 Reanalysis for Antarctic Near-Surface Air Temperature. *Atmosphere* 12(2): 217.